
ImGCL: Revisiting Graph Contrastive Learning on Imbalanced Node Classification

Liang Zeng^{1*} Lanqing Li^{2†} Ziqi Gao³ Peilin Zhao² Jian Li^{1†}

¹Institute for Interdisciplinary Information Sciences (IIIS), Tsinghua University

²Tencent AI Lab ³Hong Kong University of Science and Technology

zengl18@mails.tsinghua.edu.cn {lanqingli, masonzhao}@tencent.com

zgaoat@connect.ust.hk lijian83@mail.tsinghua.edu.cn

Abstract

Graph contrastive learning (GCL) has attracted a surge of attention due to its superior performance for learning node/graph representations without labels. However, in practice, unlabeled nodes for the given graph usually follow an implicit imbalanced class distribution, where the majority of nodes belong to a small fraction of classes (*a.k.a.*, head class) and the rest classes occupy only a few samples (*a.k.a.*, tail classes). This highly imbalanced class distribution inevitably deteriorates the quality of learned node representations in GCL. Indeed, we empirically find that most state-of-the-art GCL methods exhibit poor performance on imbalanced node classification. Motivated by this observation, we propose a principled GCL framework on Imbalanced node classification (ImGCL), which automatically and adaptively balances the representation learned from GCL without knowing the labels. Our main inspiration is drawn from the recent *progressively balanced sampling* (PBS) method in the computer vision domain. We first introduce online clustering based PBS, which balances the training sets based on pseudo-labels obtained from learned representations. We then develop the node centrality based PBS method to better preserve the intrinsic structure of graphs, which highlight the important nodes of the given graph. Besides, we theoretically consolidate our method by proving that the classifier learned by balanced sampling without labels on an imbalanced dataset can converge to the optimal balanced classifier with a linear rate. Extensive experiments on multiple imbalanced graph datasets and imbalance settings verify the effectiveness of our proposed framework, which significantly improves the performance of the recent state-of-the-art GCL methods. Further experimental ablations and analysis show that the ImGCL framework remarkably improves the representations of nodes in tail classes.

1 Introduction

Recently, graph contrastive learning (GCL) has become the *de facto standard* for self-supervised learning on graphs [1] due to its superior performance as compared to the equivalent methods trained with labels in a supervised manner on graph benchmark datasets [2–5]. Inheriting the advantage of self-supervised learning, GCL frees the model from the reliance on label information in the graph domain, where label information can be costly and error-prone in practice [6] while unlabeled/partially labeled data is extremely common, such as fraudulent user detection [7] and molecular graph data [8]. In a nutshell, most GCL methods typically first construct multiple graph views via stochastic augmentations on the input graph and then learn representations by maximizing the feature consistency between two views.

*This work was done during the first author’s internship at Tencent AI Lab.

†Corresponding authors.

Despite the proliferation and effectiveness of such methods, existing GCL methods mostly assume the standard graph benchmark datasets are carefully curated and well balanced across classes. However, unlabeled graph data randomly gathered in the wild often exhibit highly imbalanced property [9] and thus implicitly deteriorates the performance of the GCL methods [10]. For instance, Fig. 1(a) illustrates the class distribution sorted in decreasing order of the Amazon-Computers dataset [11], a network of co-purchase goods belonging to 10 classes. In the training set, we can clearly find that a small fraction of classes have massive samples (*a.k.a.*, head classes) and the rest of classes are associated with only a few samples (*a.k.a.*, tail classes). Note that the highly imbalanced property of label information within the training data is unknown to the GCL methods. This important property implicitly exists and is largely ignored by the current GCL methods [1]. On imbalanced node classification, the testing set is balanced across all classes to treat each class equally. As shown in the blue line of Fig. 1(b), we adopt one of the state-of-the-art GCL methods—GBT—to conduct experiments on imbalanced node classification settings. We can find that the baseline GBT model obtains very poor results, especially on the middle and tail classes. Hence, a natural question arises:

How to improve GCL on highly imbalanced node classification?

Recent works [12, 13] utilize progressively balanced sampling (PBS for brevity) method to decouple the learning procedure into *representation learning* and *classification* two stages and achieve remarkable success by narrowing the gap between the training and testing class distribution. However, this method is impractical since it requires knowing the labels, which does not hold in the GCL setting. This dilemma motivates us to explore how to implicitly obtain label information in the traditional GCL setting.

In this paper, we present a principled GCL framework on Imbalanced node classification (ImGCL), to automatically and adaptively balance the representation learned from GCL without knowing the labels. We first propose online clustering based PBS to implicitly obtain label information for PBS. The starting point of GCL is to push similar nodes in a given graph into the same cluster. Motivated by this, we make pseudo-labels to satisfy the need for labels in PBS. We also provide theoretical insight into our proposed method by proving that the classifier learned by balanced sampling without label information on an imbalanced dataset can converge to the optimal balanced classifier with a linear rate, which justifies the rationale of the PBS method. Moreover, we propose the node centrality based PBS method to fit the graph domain. We give large probabilities to nodes with high node centrality scores when down-sampling the head class nodes in online clustering based PBS. This scheme is able to guide the model to learn the features of nodes with high node centrality scores, which is often 'important' in the graph and has abundant structural connectivity when performing message passing. Furthermore, existing GCL models can be seamlessly incorporated into our proposed ImGCL framework. In short, our main contributions can be summarized as follows:

- *New problem and insights:* we introduce an important but under-explored problem, namely graph contrastive learning on imbalanced node classification. The recently proposed GCL methods are *vulnerable* to the imbalanced node classification setting and result in performance degradation.
- *New principled framework:* we propose a novel ImGCL framework, which utilizes the node centrality based PBS method. Further theoretical justification provides the rationale of our proposed method. Moreover, existing GCL models can be seamlessly incorporated into our framework.
- *Convincing empirical results:* we conduct comprehensive experiments to show that the ImGCL framework achieves superior performance compared with the recently proposed GCL methods

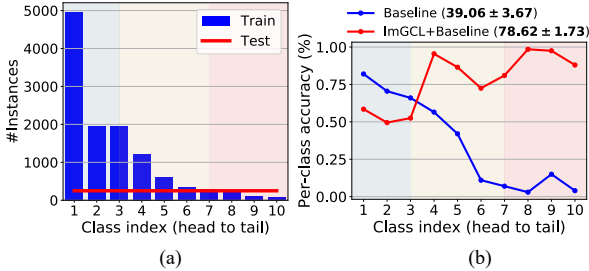


Figure 1: (a) Class distribution sorted in decreasing order of the Amazon-Computers dataset, where training sets are highly imbalanced but testing sets are balanced. (b) Compared to the GBT [3] baseline model on Amazon-computers, ImGCL+GBT substantially outperforms GBT on the overall accuracy. On three splits (many-/med-/few-shot) depicted in different colors (blue/yellow/red), ImGCL+GBT improves the performance of few- and medium-shots categories by a large margin with slightly sacrificing accuracy on many-shots.

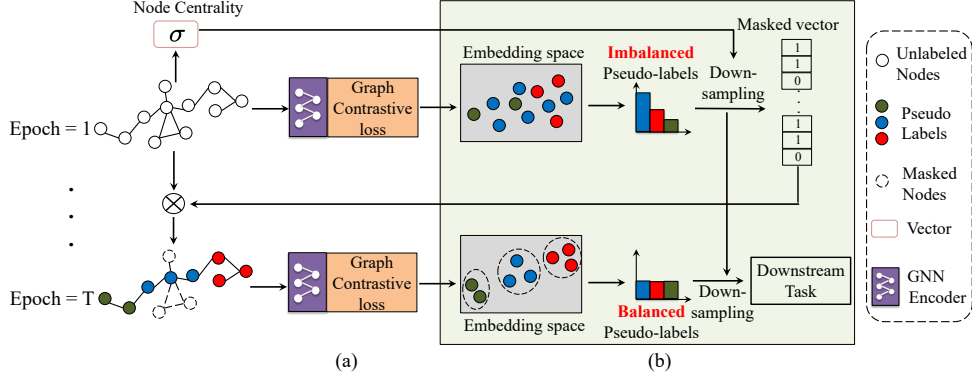


Figure 2: Overview of the proposed ImGCL framework. (a) Graph contrastive learning (GCL) methods take graph/subgraph as input and produce the corresponding node embeddings as outputs. (b) Node centrality based progressively balanced sampling (PBS) method automatically and adaptively balances the representations learned from GCL without knowing the labels.

on imbalanced node classification. Extensive ablation studies also demonstrate that the ImGCL framework improves the representations of nodes in tail classes.

2 Background

Let $\mathcal{G} = (\mathcal{V}, \mathcal{E}, \mathbf{X})$ denote a graph, where $\mathcal{V} = \{v_i\}_{i=1}^N$ is a set of N nodes, and $\mathcal{E} \subseteq \mathcal{V} \times \mathcal{V}$ is a set of edges between nodes. $\mathbf{X} = [\mathbf{x}_1, \mathbf{x}_2, \dots, \mathbf{x}_N]^T \in \mathbb{R}^{N \times d}$ represents the node feature matrix and $\mathbf{x}_i \in \mathbb{R}^d$ is the feature vector of node v_i , where d is the feature dimension. The adjacency matrix $\mathbf{A} \in \{0, 1\}^{N \times N}$ is defined by $A_{i,j} = 1$ if $(v_i, v_j) \in \mathcal{E}$ and 0 otherwise. The degree matrix $\mathbf{D} \in \mathbb{R}^{N \times N}$ is a diagonal matrix defined by $D_{ii} = \sum_j A_{ij}$.

Graph Contrastive Learning. Given an input graph, graph contrastive learning aims to learn effective graph/node representations that can be transferred to downstream tasks by constructing positive and negative sample pairs [1–3, 14–19]. GCL maximizes the feature consistency between two augmented views of the input graph via contrastive loss in the latent space [1, 4, 5]. Note that we have no access to node labels during training in the setting of GCL. However, the underlying class distribution of the unlabeled dataset is usually highly imbalanced, as shown in Fig. 1. At each training step, we first perform stochastic *graph augmentations* to generate multiple views of the original graph. Specifically, we utilize two augmentation functions $t_1, t_2 \sim \mathcal{T}$ to generate graph views $\tilde{\mathcal{G}}_1 = (\tilde{\mathbf{X}}_1, \tilde{\mathbf{A}}_1) = t_1(\mathcal{G})$ and $\tilde{\mathcal{G}}_2 = (\tilde{\mathbf{X}}_2, \tilde{\mathbf{A}}_2) = t_2(\mathcal{G})$, where \mathcal{T} is the set of graph augmentation functions, such as node dropping, edge perturbation, and subgraph sampling [5]. We then obtain node representations for the two graph views via the (parameter shared) GNN encoder $f(\cdot)$, denoted by $\mathbf{Z} = f(\tilde{\mathbf{X}}_1, \tilde{\mathbf{A}}_1)$ and $\mathbf{Z}' = f(\tilde{\mathbf{X}}_2, \tilde{\mathbf{A}}_2)$ respectively. Given the latent representations, a contrastive loss is defined to optimize the parameters of the GNN encoder. For any node u , we aim to score the positive pairs u, v higher compared to other negative pairs. Typically, the negative pairs are construed from the augmented views of the original graph or other graphs in the same batch. The commonly-used InfoNCE loss [20] can be defined as:

$$\mathcal{L}_{NCE}(u, v) = -\log \frac{s(z_u, z_v, \tau)}{s(z_u, z_v, \tau) + \sum_{n=1}^N s(z_u, z'_n, \tau)}, \quad (1)$$

where z_u and z_v denote the node representation vector of node u and v in $\tilde{\mathcal{G}}_1$, respectively. z'_n denotes the node representation of node n in $\tilde{\mathcal{G}}_2$. s is a contrasting operation to measure the similarity between two node representations. τ represents the temperature hyper-parameter. The similarity function is typically defined as: $s(z_u, z_v, \tau) = \exp(z_u \cdot z_v / \tau)$.

Imbalanced Learning. Imbalanced learning seeks to learn a model from *the training dataset with an imbalanced class distribution*, where a small fraction of classes have the vast majority of samples (*a.k.a.*, head class) and the rest classes occupy only a few samples (*a.k.a.*, tail class) [12, 21–23],

and generalize well on *the balanced testing dataset*. For a K -class node classification problem, let $\{v_i, y_i\}_{i=1}^N$ be the imbalanced training dataset, where each node v_i has the corresponding class label y_i , which is not known in the training phase of GCL. The total number of training dataset over K classes is $N = \sum_{k=1}^K N_k$, where N_k denotes the number of samples in class k . Let π be the vector of label frequencies, where $\pi_k = N_k/N$ denotes the label frequency of class k . Without loss of generality, a common assumption in imbalanced learning is that the classes are sorted by π_k in a descending order (*i.e.*, if $i_1 < i_2$, then $N_{i_1} \geq N_{i_2}$). In imbalanced learning, the number of samples in the head class is often substantially larger than that in the tail class, *i.e.*, $N_1 \gg N_K$. The imbalance ratio is defined as N_1/N_K . Note that in imbalanced learning, the training dataset is imbalanced to mimic the long-tailed class distribution of real-world data collection, but the testing dataset is balanced assuming equality of all classes. Therefore, the overall performance on all classes and the performance for the head, middle, and tail classes are usually reported.

3 ImGCL: The Proposed Framework

In this section, we first introduce the progressively balanced sampling (PBS) method, which is impractical in our unsupervised setting since it requires knowing the labels. Motivated by the property of GCL, we generate pseudo-labels by clustering the node representations. Finally, we utilize the proposed node centrality based PBS method to adaptively focus on 'important' nodes of the given graph during the down-sampling phase. The overall framework of ImGCL is shown in Fig. 2.

3.1 Progressively Balanced Sampling (PBS)

Sampling strategies. As suggested in [13], the probability p_k of sampling a node for the given graph from the class k is defined as:

$$p_k = \frac{N_k^q}{\sum_{i=1}^K N_i^q}, \quad (2)$$

where $q \in [0, 1]$. Different sampling strategies have different specific values of q .

PBS [12]. In imbalanced learning, the testing dataset is balanced whereas the training dataset is not. A single data sampling strategy which fits only one case, the balanced dataset ($p_k^M = \frac{1}{K}$ by setting $q = 0$ in Eq. 2) or the imbalanced dataset ($p_k^R = \frac{N_k}{\sum_{i=1}^K N_i}$ by setting $q = 1$ in Eq. 2), cannot account for the class distribution shift between the training and testing datasets. Thus, we adopt two data samplers with different sampling strategies for training in the imbalanced setting. The key idea is to apply an adaptive sampling strategy known as decoupled training in long-tailed learning literature [21]. Formally, at training step t , data are sampled according to a linear combination of the random and mean strategies, controlled by a parameter $\alpha \in [0, 1]$. Therefore, the probability of sampling a node from the class k is given by:

$$\begin{aligned} p_k^{\text{PB}} &= \alpha * p_k^R + (1 - \alpha) * p_k^M \\ &= \alpha * \frac{N_k}{\sum_{i=1}^K N_i} + (1 - \alpha) * \frac{1}{K}. \end{aligned} \quad (3)$$

Intuitively, at early stages of the training phase, an imbalanced class distribution is used for representation learning of the feature extractor. At later stages, the model prefers the balanced dataset for training an unbiased classifier. Therefore, the control parameter α should progressively decrease from 1 to 0 during the training phase. Concretely, at training step t , α is calculated by [12]: $\alpha = 1 - \frac{t}{T}$, where T is the total number of training epochs.

3.2 Online clustering Based PBS

Progressively balanced sampling requires real labels to adjust the class distribution during training, which compromises its practicality. Since GCL is typically applied for the label-free scenario, we cannot directly apply PBS here.

On one hand, McPherson et al. [24] have revealed the homophily phenomenon in graphs, *i.e.*, the nodes with similar features tend to be connected with each other and share the same label. On the

other hand, the motivation of GCL is to learn representations in which similar node pairs stay close to each other while dissimilar ones are far apart. We propose to connect these two facts by the pseudo-label method in semi-supervised learning [25], which iteratively generates artificial labels by the model itself to further improve its performance.

Previous work [25, 26] made a hypothesis that similar nodes may reside in the same cluster, which is far away from those dissimilar nodes, and showed that cluster assignments can be used as pseudo-labels to learn visual representations. Thus, we utilize the emergence of representation clusters learned from GCL to generate pseudo-labels of each node for the given graph. Specifically, suppose there are K -classes for the node classification task. At the certain iteration t of the training phase, we obtain the node representation $\mathbf{Z}_t \in \mathbb{R}^{N \times d}$ via the learned GNN encoder. We apply the clustering algorithm to the nodes in the embedding space to produce a set of K prototypes $\{\mathbf{c}_1, \dots, \mathbf{c}_K\}$. Formally, we intend to learn a $d \times K$ centroid matrix C and a one-hot cluster assignment vector $\hat{y}_n \in \mathbb{R}_+^K$ for each node n of the given graph by solving the following problem:

$$\min_{C \in \mathbb{R}^{d \times K}} \frac{1}{N} \sum_{n=1}^N \min_{\hat{y}_n} \|\mathbf{z}_{t,n} - C\hat{y}_n\|_2^2 \quad \text{such that} \quad \hat{y}_n^\top \mathbf{1}_K = 1 \quad , \quad (4)$$

where $\mathbf{z}_{t,n} \in \mathbb{R}^d$ denotes the n -th node embedding vector of \mathbf{Z}_t , and $\mathbf{1}_K \in \mathbb{R}^K$ is the vector with all elements of 1. Solving this above problem provides a set of optimal assignments $\{\hat{y}_n^* | n = 1, \dots, N\}$ and a centroid matrix C^* . These assignments are then used as pseudo-labels. We set the number of centroids (clusters) in the clustering algorithm equal to the number of classes in the training dataset. In order to avoid trivial solutions and empty clusters, we use the *constrained K-means clustering* [27] to instantiate the clustering algorithm. It can implement the K-means clustering algorithm whereby a minimum size for each cluster can be specified. Thus, we can address the representation collapse problem [28] which would produce a highly imbalanced pseudo-label distribution.

3.3 Node Centrality based PBS

To take full advantage of the imbalanced dataset, we propose to down-sample nodes of the head classes to balance the class distribution over all classes. We design a down-sampling strategy by incorporating graph structural information to achieve the full potential of the online clustering based PBS method. In network science, node centrality, which measures how important a node is in a graph, is an important metric to understand the influence of each node of a graph [29]. Therefore, we propose an adaptive down-sampling scheme based on node centrality when performing online clustering based PBS. In this paper, we utilize the PageRank centrality due to its simplicity and effectiveness [29]. Formally, the centrality values are calculated by the following iterative form: $\boldsymbol{\sigma} = \alpha \mathbf{A} \mathbf{D}^{-1} + \mathbf{1}$, where $\boldsymbol{\sigma} \in \mathbb{R}^N$ is the PageRank centrality score vector for each node, α is a damping factor to control the probability of randomly jumping to another node in the graph, and $\mathbf{1}$ is the identity vector with all value 1. Note that we pre-calculate the PageRank score $\boldsymbol{\sigma}$ before the training phase of GCL. When performing down-sampling of the head classes, we calculate the probability of each node based on $\boldsymbol{\sigma}$.

Formally, for node v in class j with the centrality score σ_v , the probability with the normalized centrality score is defined as: $p_{v,j}^{\text{NPB}} = \min \left\{ \frac{\sigma_{\max} - \sigma_v}{\sigma_{\max} - \sigma_{\min}} \cdot p_j^{\text{PB}}, p_\tau \right\}$, where p_j^{PB} is the progressively balanced sampling probability of class j , σ_{\max} and σ_{\min} are the maximum and minimum centrality score, and p_τ is a cut-off probability to ensure that nodes with extremely low connections can also be sampled. In node centrality based PBS, we then perform a normalization step that transforms $p_{v,j}^{\text{NPB}}$ into probabilities and then use it to balance the class distribution. Concretely, we obtain a subgraph of the original graph in form of a masked vector $\mathbf{m} \in \mathbb{R}^N$ by sampling each node independently according to p^{NPB} , which acts as the input of GCL in the next training iteration as shown in Fig. 2.

3.4 More Discussions on ImGCL

Implementation details. Instead of utilizing all nodes in the graph, we select $N \times l$ nodes in GCL, where l is a hyper-parameter to control the selected nodes. In order to consider the number of nodes in tail classes, we set $l = 10\%$ in the experiments. We down-sample the head nodes to the required number according to their PageRank centrality score. One challenge of the implementation is that the quality of the learned pseudo-labels and representations are mutually-dependent, which could

destabilize the training loop. In response, we re-balance the class distribution every B epochs, thus there are T/B times to adjust the class distribution. Following the linear evaluation scheme of GCL, we train a linear classifier with a small fraction of datasets after obtaining node representations, which is trained on the balanced dataset by using the PBS method as in [12].

Computational complexity. ImGCL is a general GCL framework. Suppose we use the traditional GCN [30] model in GCL, the training time complexity of a GCN with L layers is $\mathcal{O}(Lmd + Lnd^2)$, where d is the dimension of the learned representations, and $n = |\mathcal{V}|$ and $m = |\mathcal{E}|$ denote the number of vertices and edges in the given graph, respectively. In the ImGCL framework, the time complexity of the clustering algorithm is $\mathcal{O}(nd)$. We have $k = T/B$ times to adjust the class distribution using the clustering algorithm to produce pseudo-labels, thus we have an extra $\mathcal{O}(knd)$ time complexity. Note that k is always less than 10 in our experiments, so the time of the clustering algorithm in ImGCL is negligible compared with the training of GNN encoders of GCL. Moreover, the time complexity of calculating node centrality is $\mathcal{O}(t * n)$, where t is the number of iterations in the PageRank algorithm. This step can be seen as a pre-computing step and can also be ignored compared with the training of GNN encoders.

Modular design of ImGCL. ImGCL is a general GCL framework on imbalanced node classification, which can be readily applied with existing GCL methods adopting the two-branch design (e.g., [2–4]). ImGCL does not rely on specific approaches of graph view augmentation, graph view encoding, and representation contrasting in GCL.

4 Theoretical Justification

In order to justify our proposed method, we theoretically prove that, on the imbalanced unlabeled dataset, a classifier learned iteratively by balanced sampling converges to the optimal balanced classifier with a linear rate. Detailed proofs can be found in Appendix A.

Consider a binary classification problem with two Gaussian distributions with different means and the equal variance. Suppose the data generating distribution is P_{XY} and the probability of positive labels (+1) and negative labels (-1) are $P_Y(1)$ and $P_Y(-1)$, respectively. We have $X|Y = +1 \sim \mathcal{N}(\mu_1, \sigma^2)$ conditioned on $Y = +1$ and similarly, $X|Y = -1 \sim \mathcal{N}(\mu_2, \sigma^2)$ conditioned on $Y = -1$. In addition, suppose $\mu_1 < \mu_2$ without loss of generality. We consider the imbalanced setting and it is straightforward to have [31]:

Fact 1. *Consider the above setup, the optimal Bayes classifier is $f(x) = \text{sign}\left(x - \theta^* - \frac{\sigma^2}{\mu_2 - \mu_1} \log \frac{P_Y(1)}{P_Y(-1)}\right)$ with the optimal balanced decision boundary θ^* being $\theta^* \equiv \frac{\mu_1 + \mu_2}{2}$, where $\text{sign}(x)$ is the indicator function with $\text{sign}(x) = 1$ if $x > 0$ and -1 otherwise.*

Interpretation. Intuitively, if the label Y is either positive (+1) or negative (-1) with equal probability, the optimal Bayes’s classifier boundary is the perpendicular hyperplane through the midpoint of two Gaussian centers. However, if the number of positive labels is larger than that of negative labels, the decision boundary will be dominated by the positive (head) class and shift towards the negative (tail) class.

In the context of imbalanced learning, the training dataset is imbalanced but the testing dataset is balanced. However, in self-supervised GCL, label information is absent and we instead propose to create pseudo-labels iteratively via representations learned from GCL to enable the PBS method. At the first iteration $t = 1$, one starts from the imbalanced unlabeled dataset and generates pseudo-labels \hat{Y}_0 by the PBS method. Then, we obtain the learned decision boundary estimator $\hat{\theta}_1$ and produce pseudo-labels \hat{Y}_1 . The fact that the initial dataset being imbalanced (i.e., $P_Y(1) \neq P_Y(-1)$) leads to biased $\hat{\theta}_1$ and \hat{f}_1 by Eq. 1, which has three consequences: (1) The learned classifier \hat{f}_1 exhibits higher recall/lower precision for the head classes and the opposite for the tail classes [6], aligned with our empirical observations in Fig. 3. (2) For any iteration t , the biased classifier \hat{f}_t and pseudo-labels \hat{Y}_t induce distribution shift between the pseudo-classes \hat{X} and ground truth classes X . (3) For any following iteration t , the dataset re-balanced based on \hat{Y}_t is still imbalanced with respect to the ground truth labels Y , which by Eq. 1 means $|\hat{\theta}_{t+1} - \theta^*| > 0, \forall t \in \mathbb{N}_+$. For which we prove the following proposition:

Proposition 1. Consider the above setup. Suppose there is a (sufficiently large) integer T such that $|\hat{\theta}_T - \theta^*| \ll |\mu_2 - \mu_1|$, $|(\hat{\theta}_T - \theta^*)(\mu_2 - \mu_1)| \ll \sigma^2$. Our estimator converges to the optimal balanced decision boundary θ^* , i.e. $|\hat{\theta}_{t+1} - \theta^*| \leq C \cdot |\hat{\theta}_t - \theta^*|, \forall t \geq T$ with a linear convergence rate $C = \frac{2}{\pi} < 1$.

Interpretation. In the context of PBS, the classifier is trained starting from the imbalanced data distribution. Intuitively, by iteratively down-sampling head classes, the data distribution gradually becomes balanced, on which the trained classifier also converges to the balanced optimum. As stated in proposition 1, the classifier learned by balanced sampling with pseudo-label on the imbalanced dataset can converge to the optimal balanced classifier with a linear rate, which justifies the rationale of the PBS method.

5 Experiments

In this section, we provide empirical results to demonstrate the effectiveness of our proposed ImGCL framework. We conduct extensive experiments on imbalanced graph datasets to mainly answer the following questions: (1) Can ImGCL generally improve the performance of GCL methods on node classification? (Sec. 5.1) (2) Does all proposed components in the node centrality based PBS method benefit the learning of GCL? (Sec. 5.2) (3) How does ImGCL help improve GCL methods on imbalanced node classification? (Sec. 5.2) (4) Is ImGCL sensitive to the hyperparameters? (Sec. E)

Dataset. For a comprehensive comparison, we use four widely-used datasets, including Wiki-CS, Amazon-computers, Amazon-photo, and DBLP, to study the performance of transductive node classification. Recently proposed work evaluates the performance of semi-supervised node classification. ImGAGN [32] reconstructs the binary imbalanced network by setting the smallest class as the tail class and the rest classes as the head class. The testing dataset in Tail-GNN [9] is also imbalanced. We think these experimental settings are not ideal for imbalanced learning due to the limited number of node classes or imbalanced testing datasets. In order to validate the effectiveness of our proposed framework on the imbalanced node classification setting, we select an equal number of nodes in each class for the validation and testing dataset. The training set is randomly sampled from the rest according to train/valid/test ratios = 1:1:8, which is highly imbalanced. The statistics and the imbalance ratio of each dataset are summarized in Table 4. The detailed description of datasets can be found in Appendix F.

Evaluation protocol. For each experiment, we follow the commonly-used *linear evaluation scheme* for GCL as introduced in [5]. The model is firstly trained in a self-supervised manner, and then the learned representations are used to train and test with a simple l_2 -regularized logistic regression classifier. For results in this section, we train each model in twenty runs for different data splits and report the average performance with the corresponding standard deviation for a fair comparison. In what follows, we measure performance in terms of accuracy, if not otherwise specified.

Imbalanced types. In order to comprehensively evaluate the performance of ImGCL in different imbalanced types, we introduce two imbalanced types [10]: *Exp* and *Pareto*, parameterized by an imbalanced factor. *Exp* imbalanced class distribution is given by an exponential function, where the higher imbalanced factor means the more imbalanced graph. *Pareto* imbalanced class distribution is determined by a Pareto distribution, where the lower imbalanced factor means the smaller power value of Pareto distribution and thus the more imbalanced graph.

Baselines. We consider unsupervised baseline methods in the following two categories: (1) traditional non-GNN methods including Node2vec [33], DeepWalk [34], and raw features as input without considering the graph topology. (2) graph contrastive learning methods including DGI [16], MVGRL [18], InfoGraph [17], GRACE [5], BGRL [2], and GBT [3]. We also directly compare ImGCL with supervised counterparts, i.e., the most representative model GCN [30]. Note that for all baselines, we report their performance on the imbalanced experimental settings following their official hyperparameters (Supplement F) based on the PyGCL [1] open-source library.

5.1 Experimental Results on Node Classification

The empirical performance of imbalanced node classification is summarized in Table 1. ImGCL consistently outperforms current GCL baselines or even the supervised baselines. We summarize

Table 1: Summary of performance on imbalanced node classification in terms of accuracy (%) with standard deviation (*std*). The ‘Available Data’ means data we can obtain during the training phase, where X , A , and Y denotes the node feature matrix, the adjacency matrix, and the corresponding labels respectively. The highest performance in the GCL and ImGCL category is bold. We highlight ImGCL based on the recently proposed GCL methods with gray background. The highest performance improvement of the GCL baseline w & w/o the ImGCL framework is underlined.

Category	Method	Available Data	Amazon-Computers	Amazon-Photo	Wiki-CS	DBLP
N/A	Raw features	X	33.99 \pm 4.47	38.07 \pm 4.03	34.50 \pm 2.06	38.51 \pm 0.80
	Node2vec	A	69.80 \pm 2.69	69.44 \pm 0.38	51.76 \pm 2.24	50.41 \pm 2.77
	DeepWalk	A	69.67 \pm 2.36	69.00 \pm 0.62	51.32 \pm 2.17	50.57 \pm 2.88
	DeepWalk + features	X, A	70.20 \pm 3.30	71.60 \pm 3.31	51.51 \pm 2.51	49.57 \pm 1.65
GCL	DGI	X, A	10.88 \pm 2.09	13.62 \pm 2.26	17.11 \pm 4.83	26.63 \pm 10.87
	MVGRL	X, A	13.40 \pm 3.01	16.92 \pm 3.14	45.97 \pm 2.42	44.43 \pm 0.57
	InfoGraph	X, A	35.83 \pm 7.01	53.57 \pm 13.29	44.19 \pm 3.90	48.26 \pm 5.95
	GRACE	X, A	41.54\pm2.51	45.24 \pm 4.24	54.20\pm3.97	44.48 \pm 0.40
	BGRL	X, A	40.81 \pm 5.01	51.18 \pm 10.49	39.82 \pm 3.60	49.58 \pm 3.99
	GBT	X, A	39.06 \pm 3.67	60.73\pm3.64	<u>44.95\pm2.63</u>	58.51\pm5.30
ImGCL (ours)	DGI	X, A	48.85 \pm 10.94	47.99 \pm 9.03	41.20 \pm 18.84	50.39 \pm 9.17
	MVGRL	X, A	46.42 \pm 11.33	50.86 \pm 9.49	60.85 \pm 2.60	51.90 \pm 7.42
	InfoGraph	X, A	75.44 \pm 5.30	72.56 \pm 2.91	68.96 \pm 5.86	69.12 \pm 3.24
	GRACE	X, A	77.54 \pm 3.00	68.89 \pm 4.41	73.86\pm2.78	63.61 \pm 4.91
	BGRL	X, A	67.82 \pm 10.24	72.67 \pm 6.04	59.35 \pm 15.44	57.90 \pm 2.28
	GBT	X, A	78.62\pm1.73	75.13\pm7.13	<u>73.08\pm12.45</u>	70.05\pm1.78
Best ImGCL over GCL			39.61 \uparrow	34.47 \uparrow	28.13 \uparrow	23.76 \uparrow
Supervised	GCN	X, A, Y	46.83 \pm 1.52	68.84 \pm 2.56	59.84 \pm 2.02	51.55 \pm 2.64
	GCN+PBS	X, A, Y	70.12 \pm 9.78	73.34 \pm 8.28	63.15 \pm 5.13	73.11 \pm 2.76

our observations from the table as follows: (1) Recently proposed GCL methods [1], which are evaluated on randomly split training and testing sets, exhibit severe performance degradation in our imbalanced node classification setting. By incorporating our proposed ImGCL framework (the gray background), these GCL methods improve by a large margin. Concretely, ImGCL+GCL achieves [41.22%, 34.47%, 28.13%, 23.76%] average absolute gain in accuracy than the baseline GCL models on [Amazon-Computers, Amazon-Photo, Wiki-CS, DBLP], respectively. We also find that the recently proposed GBT [3] obtains the best performance among a set of GCL competitors. We think the reason is that *feature decorrelation* method in GBT is more fit for the imbalanced node classification and we adopt the GBT baseline model in the following experimental analysis. (2) The traditional methods, *e.g.*, Node2vec and DeepWalk, can achieve competitive performance in the imbalanced node classification task compared with GCL methods. We postulate the reason is that the traditional network embedding methods can take advantage of the homophily [29] property of the given graph to utilize the graph topology features which is important on imbalanced node classification [9]. Moreover, the ‘‘Raw features’’ method without considering the graph topology features on imbalanced node classification. (3) Compared with the supervised learning methods GCN and GCN+PBS, the ImGCL framework achieves superior or competitive performance on all datasets, which further corroborates the effectiveness of our proposed framework.

5.2 Experimental Analysis

Imbalanced type analysis. In the imbalanced node classification setting, the performance for the head, middle, and tail classes are usually reported [21]. We first divide the Amazon-computers dataset into three disjoint groups in terms of class size: *Many*, *Medium*, *Few*. *Many* and *Few* each include the top and bottom 1/3 classes, respectively. Because there are 10 classes of Amazon-computers in total, the classes with sorted indices in decreasing order [1-3, 4-7, 8-10] belong to [*Many* (3 classes), *Medium* (4 classes), *Few* (3 classes)] categories, respectively. To validate our proposed model across different imbalanced class distributions, we design experiments on Amazon-computers using the GBT baseline model w & w/o the ImGCL framework. We consider two imbalanced types: Exp and Pareto. Four imbalanced factors [20, 50, 100, 200] are associated with Exp. Two imbalance factors [1, 2] are chosen for Pareto. In Table 2, we observe that the more imbalanced dataset leads to decreasing accuracy of the model. Intuitively, according to Eq. 1, a too imbalanced

Table 2: Results of accuracy (%) on Amazon-computers using the GBT baseline model under different imbalanced types and factors. \uparrow means higher imbalanced factor corresponds to more imbalanced dataset. Instead, \downarrow means lower factor corresponds to more imbalanced dataset. All models are trained for eight iterations of pseudo labeling.

Imbalanced type	Imbalanced factor	Method category	Many	Medium	Few	All
Exp \uparrow	20	GBT	79.67 \pm 3.59	72.82 \pm 6.37	65.64 \pm 4.52	71.97 \pm 3.78
	50		80.04 \pm 2.91	62.74 \pm 3.35	47.48 \pm 7.92	65.49 \pm 3.37
	100		72.84 \pm 5.96	29.13 \pm 3.58	7.30 \pm 3.65	39.06 \pm 3.67
	200		79.08 \pm 2.56	24.42 \pm 4.61	6.21 \pm 3.28	36.57 \pm 4.30
Pareto \downarrow	20	GBT+ImGCL (ours)	72.05 \pm 7.77	90.08 \pm 5.20	93.58 \pm 3.36	85.82 \pm 1.99
	50		64.47 \pm 11.73	86.12 \pm 9.92	93.49 \pm 3.83	82.30 \pm 3.69
	100		58.17 \pm 7.29	83.88 \pm 8.46	94.67 \pm 6.07	78.62 \pm 1.73
	200		52.95 \pm 17.70	74.26 \pm 18.75	88.58 \pm 18.19	67.12 \pm 8.14
Pareto \downarrow	2	GBT	83.33 \pm 1.42	61.00 \pm 1.07	52.57 \pm 9.05	65.17 \pm 1.66
	1		81.98 \pm 1.44	57.47 \pm 2.01	39.58 \pm 7.25	59.46 \pm 1.74
	2	GBT+ImGCL (ours)	49.10 \pm 3.19	69.94 \pm 2.41	89.98 \pm 2.13	72.20 \pm 0.78
	1		41.45 \pm 4.75	79.04 \pm 2.84	86.86 \pm 3.06	70.31 \pm 1.38

dataset might break our assumption in Proposition 1 that $|\hat{\theta}_t - \theta^*| \ll |\mu_2 - \mu_1|$, which undermines the convergence guarantee and therefore degrades performance of ImGCL given a fixed number of iterations. Nevertheless, the ImGCL+baseline model consistently outperforms the baseline model.

Per-class analysis. We analyze the per-class recall and precision in Fig. 3 to better understand the model bias on the imbalanced node classification. We test GBT on Amazon-computers under imbalanced experimental settings introduced in Sec. 5. The GBT baseline model exhibits highly skewed performance on head and tail classes. The recall on the most majority and minority class is 82.0% and 4.1% respectively, while the corresponding numbers for precision are 30.9% and 95.8%. We observe that GBT falsely classifies most of the tail class samples into head classes with low confidence but have high confidence on the correctly classified nodes in tail classes [35]. In contrast, GBT with ImGCL obtains relatively balanced recall and precision value on both head (the most majority precision: 30.9% \rightarrow 81.2%) and tail (the most minority recall: 4.1% \rightarrow 88.2%) classes, which leads to the substantial improvement in the overall accuracy (*i.e.*, 39.06% \rightarrow 78.62%) across all classes, as shown in Table 3.

Visualization. For a more intuitive comparison and to further demonstrate the effectiveness of the ImGCL framework, we design experiments of visualization on Amazon-computers. We utilize the output embeddings on the last layer of GBT w & w/o ImGCL before *softmax* and plot the learned representation of the testing graph dataset using t-SNE [36]. As in Fig. 4, GBT w/o ImGCL clearly exhibits minority collapse [28]. In Fig. 4 (a), where the representations in tail classes are mixed together, which fundamentally limits the performance of the baseline model on the tail classes. In com-

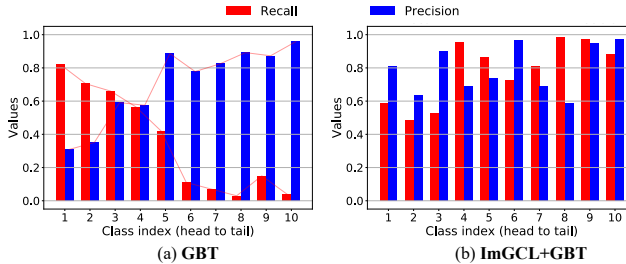


Figure 3: Bias comparison between GBT models w & w/o ImGCL on Amazon-Computers under imbalanced experimental settings. *Left:* Per-class recall and precision w/o ImGCL. *Right:* Per-class recall and precision with ImGCL. The class index is sorted by the number of nodes in each class in descending order. GBT w/o ImGCL clearly shows a descending trend in recall while an ascending trend in precision. However, GBT with ImGCL has achieved a relatively balanced recall and precision value over all classes.

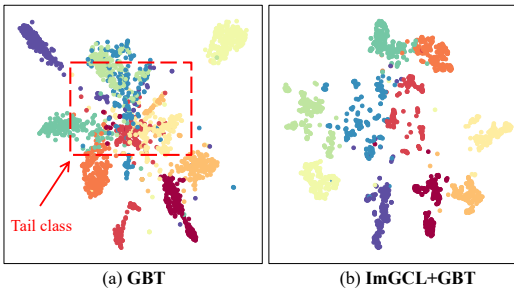


Figure 4: Visualization of the testing set on Amazon-Computers. Each point in the figure is colored by real labels.

parison, the learned embeddings of GBT+ImGCL has distinct boundaries among different classes and more compact intra-class structures.

6 Conclusion

In this work, we study how to improve graph contrastive learning methods on imbalanced node classification, which is a very practical but rarely explored problem. We propose the principled ImGCL framework, which automatically and adaptively balances the representation learned from GCL without knowing the classes and then theoretically justifies it. Through extensive experiments on multiple graph datasets and imbalance settings, we show that ImGCL can significantly improve the recently proposed GCL methods by improving the representations of nodes in tail classes. For the future work, we will explore more data types, such as bioinformatics graphs. We hope our work will extend GCL to more realistic task settings with (underlying) imbalanced node class distribution.

References

- [1] Yanqiao Zhu, Yichen Xu, Qiang Liu, and Shu Wu. An empirical study of graph contrastive learning. In *Thirty-fifth Conference on Neural Information Processing Systems Datasets and Benchmarks Track*, 2021.
- [2] Shantanu Thakoor, Corentin Tallec, Mohammad Gheshlaghi Azar, Rémi Munos, Petar Veličković, and Michal Valko. Large-scale representation learning on graphs via bootstrapping. In *International Conference on Learning Representations (ICLR)*, 2022.
- [3] Piotr Bielak, Tomasz Kajdanowicz, and Nitesh V Chawla. Graph barlow twins: A self-supervised representation learning framework for graphs. *arXiv preprint arXiv:2106.02466*, 2021.
- [4] Yuning You, Tianlong Chen, Yongduo Sui, Ting Chen, Zhangyang Wang, and Yang Shen. Graph contrastive learning with augmentations. In *Advances in neural information processing systems (NeurIPS)*, 2020.
- [5] Yanqiao Zhu, Yichen Xu, Feng Yu, Qiang Liu, Shu Wu, and Liang Wang. Graph contrastive learning with adaptive augmentation. In *Proceedings of the Web Conference (WWW)*, pages 2069–2080, 2021.
- [6] Yuzhe Yang and Zhi Xu. Rethinking the value of labels for improving class-imbalanced learning. In *Thirty-Fourth Advances in Neural Information Processing Systems (NeurIPS)*, 2020.
- [7] Srijan Kumar, Bryan Hooi, Disha Makhija, Mohit Kumar, Christos Faloutsos, and VS Subrahmanian. Rev2: Fraudulent user prediction in rating platforms. In *Proceedings of the Eleventh ACM International Conference on Web Search and Data Mining*, pages 333–341, 2018.
- [8] Hehuan Ma, Yatao Bian, Yu Rong, Wenbing Huang, Tingyang Xu, Weiyang Xie, Geyan Ye, and Junzhou Huang. Multi-view graph neural networks for molecular property prediction. *arXiv preprint arXiv:2005.13607*, 2020.
- [9] Zemin Liu, Trung-Kien Nguyen, and Yuan Fang. Tail-gnn: Tail-node graph neural networks. In *Proceedings of the 27th ACM SIGKDD Conference on Knowledge Discovery & Data Mining*, pages 1109–1119, 2021.
- [10] Ziyu Jiang, Tianlong Chen, Bobak Mortazavi, and Zhangyang Wang. Self-damaging contrastive learning. In *International Conference on Machine Learning*, 2021.
- [11] Oleksandr Shchur, Maximilian Mumme, Aleksandar Bojchevski, and Stephan Günnemann. Pitfalls of graph neural network evaluation. *arXiv preprint arXiv:1811.05868*, 2018.
- [12] Bingyi Kang, Saining Xie, Marcus Rohrbach, Zhicheng Yan, Albert Gordo, Jiashi Feng, and Yannis Kalantidis. Decoupling representation and classifier for long-tailed recognition. In *8th International Conference on Learning Representations (ICLR)*, 2020.
- [13] Ju He, Adam Kortylewski, Shaokang Yang, Shuai Liu, Cheng Yang, Changhu Wang, and Alan Yuille. Rethinking re-sampling in imbalanced semi-supervised learning. *arXiv preprint arXiv:2106.00209*, 2021.

- [14] Hengrui Zhang, Qitian Wu, Junchi Yan, David Wipf, and Philip S Yu. From canonical correlation analysis to self-supervised graph neural networks. In *Advances in Neural Information Processing Systems (NeurIPS)*, 2021.
- [15] Dongkuan Xu, Wei Cheng, Dongsheng Luo, Haifeng Chen, and Xiang Zhang. Infogcl: Information-aware graph contrastive learning. *Advances in Neural Information Processing Systems*, 34, 2021.
- [16] Petar Veličković, William Fedus, William L Hamilton, Pietro Liò, Yoshua Bengio, and R Devon Hjelm. Deep graph infomax. In *Proceedings of the International Conference on Learning Representations (ICLR)*, 2018.
- [17] Fan-Yun Sun, Jordan Hoffmann, Vikas Verma, and Jian Tang. Infograph: Unsupervised and semi-supervised graph-level representation learning via mutual information maximization. In *Proceedings of the International Conference on Learning Representations (ICLR)*, 2020.
- [18] Kaveh Hassani and Amir Hosein Khasahmadi. Contrastive multi-view representation learning on graphs. In *International Conference on Machine Learning*, pages 4116–4126. PMLR, 2020.
- [19] Jiezhong Qiu, Qibin Chen, Yuxiao Dong, Jing Zhang, Hongxia Yang, Ming Ding, Kuansan Wang, and Jie Tang. Gcc: Graph contrastive coding for graph neural network pre-training. In *Proceedings of the 26th ACM SIGKDD International Conference on Knowledge Discovery & Data Mining*, pages 1150–1160, 2020.
- [20] Ben Poole, Sherjil Ozair, Aaron Van Den Oord, Alex Alemi, and George Tucker. On variational bounds of mutual information. In *International Conference on Machine Learning*, pages 5171–5180. PMLR, 2019.
- [21] Yifan Zhang, Bingyi Kang, Bryan Hooi, Shuicheng Yan, and Jiashi Feng. Deep long-tailed learning: A survey. *arXiv preprint arXiv:2110.04596*, 2021.
- [22] Yongshun Zhang, Xiu-Shen Wei, Boyan Zhou, and Jianxin Wu. Bag of tricks for long-tailed visual recognition with deep convolutional neural networks. In *Proceedings of the AAAI Conference on Artificial Intelligence*, volume 35, pages 3447–3455, 2021.
- [23] Ziwei Liu, Zhongqi Miao, Xiaohang Zhan, Jiayun Wang, Boqing Gong, and Stella X Yu. Large-scale long-tailed recognition in an open world. In *Proceedings of the IEEE/CVF Conference on Computer Vision and Pattern Recognition*, pages 2537–2546, 2019.
- [24] Miller McPherson, Lynn Smith-Lovin, and James M Cook. Birds of a feather: Homophily in social networks. *Annual review of sociology*, 27(1):415–444, 2001.
- [25] Mathilde Caron, Piotr Bojanowski, Armand Joulin, and Matthijs Douze. Deep clustering for unsupervised learning of visual features. In *Proceedings of the European Conference on Computer Vision (ECCV)*, pages 132–149, 2018.
- [26] Mathilde Caron, Ishan Misra, Julien Mairal, Priya Goyal, Piotr Bojanowski, and Armand Joulin. Unsupervised learning of visual features by contrasting cluster assignments. In *Thirty-Fourth Advances in Neural Information Processing Systems (NeurIPS)*, 2020.
- [27] Paul S Bradley, Kristin P Bennett, and Ayhan Demiriz. Constrained k-means clustering. *Microsoft Research, Redmond*, 20(0):0, 2000.
- [28] Cong Fang, Hangfeng He, Qi Long, and Weijie J Su. Exploring deep neural networks via layer-peeled model: Minority collapse in imbalanced training. *Proceedings of the National Academy of Sciences*, 118(43), 2021.
- [29] Albert-László Barabási. Network science. *Philosophical Transactions of the Royal Society A: Mathematical, Physical and Engineering Sciences*, 371(1987):20120375, 2013.
- [30] Thomas N Kipf and Max Welling. Semi-supervised classification with graph convolutional networks. In *Proceedings of the International Conference on Learning Representations (ICLR)*, 2016.

- [31] Christopher M Bishop and Nasser M Nasrabadi. *Pattern recognition and machine learning*, volume 4. Springer, 2006.
- [32] Liang Qu, Huaisheng Zhu, Ruiqi Zheng, Yuhui Shi, and Hongzhi Yin. Imgagn: Imbalanced network embedding via generative adversarial graph networks. In *Proceedings of the 27th ACM SIGKDD Conference on Knowledge Discovery & Data Mining (KDD)*, 2021.
- [33] Aditya Grover and Jure Leskovec. node2vec: Scalable feature learning for networks. In *Proceedings of the 22nd ACM SIGKDD international conference on Knowledge discovery and data mining*, pages 855–864, 2016.
- [34] Bryan Perozzi, Rami Al-Rfou, and Steven Skiena. Deepwalk: Online learning of social representations. In *Proceedings of the 20th ACM SIGKDD international conference on Knowledge discovery and data mining*, pages 701–710, 2014.
- [35] Chen Wei, Kihyuk Sohn, Clayton Mellina, Alan Yuille, and Fan Yang. Crest: A class-rebalancing self-training framework for imbalanced semi-supervised learning. In *Proceedings of the IEEE/CVF Conference on Computer Vision and Pattern Recognition*, pages 10857–10866, 2021.
- [36] Laurens Van der Maaten and Geoffrey Hinton. Visualizing data using t-sne. *Journal of machine learning research*, 9(11), 2008.
- [37] Chenxin Tao, Honghui Wang, Xizhou Zhu, Jiahua Dong, Shiji Song, Gao Huang, and Jifeng Dai. Exploring the equivalence of siamese self-supervised learning via a unified gradient framework. In *IEEE Conference on Computer Vision and Pattern Recognition (CVPR)*, 2021.
- [38] Ting Chen, Simon Kornblith, Mohammad Norouzi, and Geoffrey Hinton. A simple framework for contrastive learning of visual representations. In *International conference on machine learning*, pages 1597–1607. PMLR, 2020.
- [39] Albert-László Barabási and Réka Albert. Emergence of scaling in random networks. *science*, 286(5439):509–512, 1999.
- [40] Tianxiang Zhao, Xiang Zhang, and Suhang Wang. Graphsmote: Imbalanced node classification on graphs with graph neural networks. In *Proceedings of the 14th ACM International Conference on Web Search and Data Mining*, pages 833–841, 2021.
- [41] Nitesh V Chawla, Kevin W Bowyer, Lawrence O Hall, and W Philip Kegelmeyer. Smote: synthetic minority over-sampling technique. *Journal of artificial intelligence research*, 16: 321–357, 2002.
- [42] Zemin Liu, Wentao Zhang, Yuan Fang, Xinming Zhang, and Steven CH Hoi. Towards locality-aware meta-learning of tail node embeddings on networks. In *Proceedings of the 29th ACM International Conference on Information & Knowledge Management*, pages 975–984, 2020.
- [43] Yu Wang, Charu Aggarwal, and Tyler Derr. Distance-wise prototypical graph neural network in node imbalance classification. *arXiv preprint arXiv:2110.12035*, 2021.
- [44] Min Shi, Yufei Tang, Xingquan Zhu, David Wilson, and Jianxun Liu. Multi-class imbalanced graph convolutional network learning. In *Proceedings of the Twenty-Ninth International Joint Conference on Artificial Intelligence (IJCAI-20)*, 2020.
- [45] William L Hamilton. Graph representation learning. *Synthesis Lectures on Artificial Intelligence and Machine Learning*, 14(3):1–159, 2020.

A Mathematics Proof

A.1 Proof of Fact 1

The optimal Bayes's classifier is the probabilistic model that makes the most probable prediction for new examples. Thus, we have:

$$\begin{aligned} f^*(x) &= \arg \max_y P_{Y|X}(y|x) \\ &= \arg \max_y P_{X|Y}(x|y)P_Y(y), \end{aligned} \quad (5)$$

where we omit $P_X(x)$ in the denominator, which is unrelated to the objective function. Due to the monotonicity property of the \log function, we have:

$$\begin{aligned} f^*(x) &= \arg \max_y \{\log P_{X|Y}(x|y) + \log P_Y(y)\} \\ &= \arg \max_y \left\{ \log \left[\frac{1}{\sqrt{2\pi\sigma^2}} \exp \left\{ -\frac{(x - \mu_y)^2}{2\sigma^2} \right\} \right] + \log P_Y(y) \right\} \\ &= \arg \min_y \left\{ \frac{(x - \mu_y)^2}{2\sigma^2} - \log P_Y(y) \right\} \\ &= \arg \min_y \left\{ -2x\mu_y + \mu_y^2 - 2\sigma^2 \log P_Y(y) \right\}. \end{aligned} \quad (6)$$

So, we will pick the positive sample +1 if

$$\begin{aligned} -2x\mu_1 + \mu_1^2 - 2\sigma^2 \log P_Y(1) &< -2x\mu_2 + \mu_2^2 - 2\sigma^2 \log P_Y(-1) \\ \Rightarrow 2x(\mu_2 - \mu_1) &< \mu_2^2 - \mu_1^2 + 2\sigma^2 \log \frac{P_Y(1)}{P_Y(-1)} \quad (\text{because of } \mu_1 < \mu_2) \\ \Rightarrow x &< \frac{\mu_1 + \mu_2}{2} + \frac{\sigma^2}{\mu_2 - \mu_1} \log \frac{P_Y(1)}{P_Y(-1)}. \end{aligned} \quad (7)$$

Therefore, the optimal Bayes's classifier is:

$$f^*(x) = \text{sign} \left(x - \frac{\mu_1 + \mu_2}{2} - \frac{\sigma^2}{\mu_2 - \mu_1} \log \frac{P_Y(1)}{P_Y(-1)} \right), \quad (8)$$

where sign is the indicator function with $\text{sign}(x) = 1$ if $x > 0$ and $\text{sign}(x) = -1$ otherwise.

A.2 Proof of Proposition 1

At training step t , we obtain the biased decision boundary $\hat{\theta}_t$ and generate corresponding pseudo-labels \hat{Y}_t . We perform the balanced sampling method on \hat{Y}_t to get balanced positive and negative samples and then take them as input for the next training step to get $\hat{\theta}_{t+1}$. Suppose the probability of true labels on selected positive samples (+1) and negative samples (-1) are $P_{Y,t}(1)$ and $P_{Y,t}(-1)$, respectively. According to Fact 1, the decision boundary $\hat{\theta}_t$ produces the bias term $\Delta = \frac{\sigma^2}{\mu_2 - \mu_1} \log \frac{P_{Y,t}(1)}{P_{Y,t}(-1)}$. We intend to prove that, at training step $t + 1$, we get a smaller bias term $C\Delta$, where $C < 1$. Without loss of generality, we set $\sigma = 1$ in what follows, which can be recovered by dimensional analysis. The optimal balanced decision boundary is $\theta^* = \frac{\mu_1 + \mu_2}{2}$, and we construct the estimator $\hat{\theta}_{t+1} = \frac{\hat{\mu}_{t,1} + \hat{\mu}_{t,2}}{2}$ by the balanced sampling method. Therefore, we need to estimate $\hat{\mu}_{t,1}$ and $\hat{\mu}_{t,2}$ conditional on the decision boundary $\hat{\theta}_t$. Suppose the cumulative distribution function (CDF) of the standard normal distribution with a mean of 0 and standard deviation of 1 is $\Phi(\cdot)$. For clarity, we denote $x = \frac{\mu_2 - \mu_1}{2} > 0$ assuming $\mu_1 < \mu_2$ and $A = \frac{1}{\sqrt{2\pi}} e^{-\frac{x^2}{2}}$. The imbalanced ratio of positive and negative samples is defined as:

$$\frac{p_{Y,t}(1)}{p_{Y,t}(-1)} = e^{\Delta(\mu_2 - \mu_1)}. \quad (9)$$

Since $\Delta = |\hat{\theta}_t - \theta^*|$ satisfies $\Delta \ll |\mu_2 - \mu_1|$ and $|\Delta(\mu_2 - \mu_1)| \ll \sigma^2 = 1$, we have the following equation by first-order approximation:

$$\begin{aligned} e^{-(x+\Delta)^2} &\approx e^{-x^2} - 2xe^{-x^2} * \Delta \\ \Phi(x + \Delta) &\approx \Phi(x) + \Phi'(x) * \Delta \\ &= \Phi(x) + \frac{1}{\sqrt{2\pi}} e^{-\frac{x^2}{2}} * \Delta. \end{aligned} \quad (10)$$

The probability of $Y = 1$ on the left of the decision boundary $\hat{\theta}_t$ is:

$$\begin{aligned} \Phi\left(\frac{\mu_1 + \mu_2}{2} - \mu_1 + \Delta\right) P_{Y,t}(1) &= \Phi\left(\frac{\mu_2 - \mu_1}{2} + \Delta\right) P_{Y,t}(1) \\ &= \Phi(x + \Delta) P_{Y,t}(1). \end{aligned} \quad (11)$$

The probability of $Y = -1$ on the left of the decision boundary $\hat{\theta}_t$ is:

$$\Phi\left(\frac{\mu_1 + \mu_2}{2} - \mu_2 + \Delta\right) P_{Y,t}(-1) = \Phi(-x + \Delta) P_{Y,t}(-1). \quad (12)$$

The total probability mass on the left of the decision boundary $\hat{\theta}_t$ is:

$$D_L = \Phi(x + \Delta) P_{Y,t}(1) + \Phi(-x + \Delta) P_{Y,t}(-1) \quad (13)$$

$$= [\Phi(x) + A\Delta] P_{Y,t}(1) + [\Phi(-x) + A\Delta] P_{Y,t}(-1). \quad (14)$$

By translating the Gaussian to zero mean, the unnormalized mean of $Y = 1$ on the left of the decision boundary $\hat{\theta}_t$ is:

$$\begin{aligned} &\left[\mu_1 \Phi(x + \Delta) + \frac{1}{\sqrt{2\pi}} \int_{-\infty}^{x+\Delta} x e^{-\frac{x^2}{2}} dx \right] P_{Y,t}(1) \\ &= \left[\mu_1 \Phi(x + \Delta) - \frac{1}{\sqrt{2\pi}} e^{-\frac{(x+\Delta)^2}{2}} \right] P_{Y,t}(1) \\ &= [\mu_1 (\Phi(x) + A\Delta) - A + Ax\Delta] P_{Y,t}(1). \end{aligned} \quad (15)$$

Similarly, the unnormalized mean of $Y = -1$ on the left of the decision boundary $\hat{\theta}_t$ is:

$$\begin{aligned} &\left[\mu_2 \Phi(-x + \Delta) + \frac{1}{\sqrt{2\pi}} \int_{-\infty}^{-x+\Delta} x e^{-\frac{x^2}{2}} dx \right] P_{Y,t}(-1) \\ &= \left[\mu_2 \Phi(-x + \Delta) - \frac{1}{\sqrt{2\pi}} e^{-\frac{(-x+\Delta)^2}{2}} \right] P_{Y,t}(-1) \\ &= [\mu_2 (\Phi(-x) + A\Delta) - A - Ax\Delta] P_{Y,t}(-1). \end{aligned} \quad (16)$$

The estimated mean on the left of the decision boundary is given by N_L/D_L where:

$$\begin{aligned} N_L &= [\mu_1 (\Phi(x) + A\Delta) - A + Ax\Delta] P_{Y,t}(1) \\ &\quad + [\mu_2 (\Phi(-x) + A\Delta) - A - Ax\Delta] P_{Y,t}(-1). \end{aligned} \quad (17)$$

According to Eq. 9, we have $\frac{p_{Y,t}(1)}{p_{Y,t}(-1)} = e^{\Delta(\mu_2 - \mu_1)} \approx 1 + \Delta(\mu_2 - \mu_1)$. Dividing both N_L and D_L by $P_{Y,t}(-1)$, we have:

$$\begin{aligned} D_L &= [\Phi(x) + A\Delta] [1 + \Delta(\mu_2 - \mu_1)] + [\Phi(-x) + A\Delta] \\ N_L &= [\mu_1 (\Phi(x) + A\Delta) - A + Ax\Delta] [1 + \Delta(\mu_2 - \mu_1)] \\ &\quad + [\mu_2 (\Phi(-x) + A\Delta) - A - Ax\Delta]. \end{aligned} \quad (18)$$

Similarly, on the right of the decision boundary, we get:

$$\begin{aligned} D_R &= [\Phi(-x) - A\Delta] [1 + \Delta(\mu_2 - \mu_1)] + [\Phi(x) - A\Delta] \\ N_R &= [\mu_1 (\Phi(-x) - A\Delta) + A - Ax\Delta] [1 + \Delta(\mu_2 - \mu_1)] \\ &\quad + [\mu_2 (\Phi(x) - A\Delta) + A + Ax\Delta]. \end{aligned} \quad (19)$$

Next, we can estimate $\hat{\mu}_{t,1}$ and $\hat{\mu}_{t,2}$ according to Eq. 18 and 19.

$$\begin{aligned}\hat{\mu}_{t,1} &= \frac{N_L}{D_L} = \frac{[\mu_1\Phi(x) - 2A + \mu_2\Phi(-x)] + \Delta\mu_1 [2A + (\mu_2 - \mu_1)\Phi(x)]}{1 + \Delta [2A + (\mu_2 - \mu_1)\Phi(x)]} \\ &= \{[\mu_1\Phi(x) - 2A + \mu_2\Phi(-x)] + \Delta\mu_1 [2A + (\mu_2 - \mu_1)\Phi(x)]\} \\ &\quad * \{1 - \Delta [2A + (\mu_2 - \mu_1)\Phi(x)]\} \\ &= [\mu_1\Phi(x) - 2A + \mu_2\Phi(-x)] \\ &\quad + \Delta [2A + (\mu_2 - \mu_1)\Phi(x)] [2A - (\mu_2 - \mu_1)\Phi(-x)],\end{aligned}\tag{20}$$

$$\begin{aligned}\hat{\mu}_{t,2} &= \frac{N_R}{D_R} = \frac{[\mu_1\Phi(-x) + 2A + \mu_2\Phi(x)] + \Delta\mu_1 [-2A + (\mu_2 - \mu_1)\Phi(-x)]}{1 + \Delta [-2A + (\mu_2 - \mu_1)\Phi(-x)]} \\ &= \{[\mu_1\Phi(-x) + 2A + \mu_2\Phi(x)] + \Delta\mu_1 [-2A + (\mu_2 - \mu_1)\Phi(-x)]\} \\ &\quad * \{1 - \Delta [-2A + (\mu_2 - \mu_1)\Phi(-x)]\} \\ &= [\mu_1\Phi(-x) + 2A + \mu_2\Phi(x)] \\ &\quad + \Delta [2A - (\mu_2 - \mu_1)\Phi(-x)] [2A + (\mu_2 - \mu_1)\Phi(x)],\end{aligned}\tag{21}$$

where we use the property of the Φ function, *i.e.*, $\Phi(x) = 1 - \Phi(-x)$. Then, we have:

$$\begin{aligned}\hat{\theta}_{t+1} &= \frac{\hat{\mu}_{t,1} + \hat{\mu}_{t,2}}{2} = \frac{1}{2} \left(\frac{N_L}{D_L} + \frac{N_R}{D_R} \right) \\ &= \frac{\mu_1 + \mu_2}{2} + \Delta [2A + (\mu_2 - \mu_1)\Phi(x)] [2A - (\mu_2 - \mu_1)\Phi(-x)].\end{aligned}\tag{22}$$

Finally, we can get:

$$\begin{aligned}C &= [2A + (\mu_2 - \mu_1)\Phi(x)] [2A - (\mu_2 - \mu_1)\Phi(-x)] \\ &= (2A + 2x\Phi(x))(2A - 2x\Phi(-x)) \\ &= 4(A + x\Phi(x))(A - x(1 - \Phi(x))) \\ &= 4(A^2 + Ax(2\Phi(x) - 1) - x^2\Phi(x)(1 - \Phi(x))), x \geq 0.\end{aligned}\tag{23}$$

We can verify that when $x = 0$, one obtains the maximal value $C = 4A^2 = \frac{2}{\pi} \approx 0.637 < 1$. This completes the proof.

B More Discussions on Graph Contrastive Learning and Imbalanced Learning

Graph Contrastive Learning. Some recent remarkable progress has been made to adapt contrastive learning methods to the graph domain. Typically, the main idea behind graph contrastive learning (GCL) is to learn effective representations in which similar sample pairs stay close to each other while dissimilar ones are far apart [1]. According to [37], we can divide GCL methods into three categories: (1) *contrastive learning* methods [16–18, 4, 5] aim to reduce the distance between two augmented views of the same nodes/graphs (positive samples), and push apart views of different nodes/graphs (negative samples). These methods mainly differ in several design choices including graph data augmentations, contrasting modes, and contrastive objectives. DGI [16] adopts the InfoNCE principle [20] to the node classification task by contrasting the node- and graph-level representations of the given graph. InfoGraph [17] mainly focus on graph classification task by contrasting graph representation of different granularity via mutual information maximization. MV-GRL [18] utilizes the graph diffusion matrix to construct the augmentation views of the original graph and then contrast node- and graph-level representation by scoring the agreement between representations. GraphCL [4] adopts the SimCLR [38] framework and propose four practical graph augmentation methods to obtain better graph representations. GRACE [5] capitalizes on the idea that data augmentations for GCL should preserve the property of graphs to highlight important node features. (2) Negative samples play an important role in contrastive learning methods. However, *asymmetric network* methods [2] get rid of negative samples via the introduction of a predictor network and the stop-gradient operation to avoid mode collapse. (3) *Feature decorrelation* methods [14, 3] has recently been introduced as a new solution to GCL. They focus on reducing the redundancy among feature dimensions by introducing a loss function calculated by the cross-correlation matrix

of two augmentation views. Different from our work, these methods mainly assume that the unlabeled graph data distribution is always balanced for GCL. However, in practice, the (unlabeled) class distribution could be highly skewed and lead to sub-optimal generalization on the imbalanced graph dataset.

Imbalanced Learning. It is well known that the degree of many large graphs follows a scale-free power-law distribution, which is long-tailed and highly imbalanced [39]. In this work, we focus on the imbalanced class distribution, which is also ubiquitous for graph datasets. There exists some recent work to study the class imbalance of semi-supervised node classification problems. They mainly improve the imbalanced classification performance by re-balancing the sample ratio of head and tail classes [40, 32, 41] and transfer knowledge from head classes to enhance model performance on tail classes [42–44]. GraphSMOTE [40] utilizes the SMOTE synthetic over-sampling algorithm to up-sample the tail nodes and then improve their prediction performance. ImGAGN [32] aims to improve the representation learning of tail nodes by generating adversarial tail nodes to balance the class distribution of the original graph. DPGNN [43] borrows the idea of metric learning to transfer knowledge from head classes to tail classes to boost model performance. However, they mainly ignore that open-world unlabeled data usually follows the imbalanced distribution, which will lead to performance degradation under unsupervised or self-supervised learning. To our best knowledge, we are the first to explore contrastive learning on *highly* imbalanced graph datasets.

C More Discussions on Data Sampling Strategies

Different sampling strategies have different specific values of q in Eq. 2, which have different practical meanings introduced below.

Random sampling. The probability of a node from the class k is defined as $p_k^R = \frac{N_k}{\sum_{i=1}^K N_i}$ by setting $q = 1$ in Eq. 2, referred to as instance-balanced sampling in some literature [21]. A node from class k is sampled proportionally according to the cardinality N_k of each class. If we sample nodes from a given graph according to p_k^R , the highly imbalanced property still remains just like the training dataset in imbalanced learning. It reflects the highly imbalanced and skewed class distribution of real-world data collection.

Mean sampling. The probability of a node from the class k is given by $p_k^M = \frac{1}{K}$ by setting $q = 0$ in Eq. 2, referred to as class-balanced sampling in some literature [21]. A node is sampled with an equal probability for each class. Sampling each class with an equal probability according to p_k^M has been found to significantly improve the performance of the classifier in long-tailed learning, while being sub-optimal for representation learning [12].

D Ablation Study on Amazon-computers

We conduct ablations using the GBT baseline on Amazon-computers due to its largest imbalanced factor among four datasets, as shown in Tabel 4. In the imbalanced node classification setting, the performance for the head, middle, and tail classes are usually reported [21]. We first divide the Amazon-computers dataset into three disjoint groups in terms of class size: *Many*, *Medium*, *Few*. *Many* and *Few* each include the top and bottom 1/3 classes, respectively. Because there are 10 classes of Amazon-computers in total, the classes with sorted indices in decreasing order [1-3, 4-7, 8-10] belong to [*Many* (3 classes), *Medium* (4 classes), *Few* (3 classes)] categories, respectively. We consider four variants of GBT+ImGCL in three settings: GBT with one-stage pseudo-labels (k-means and community detection), multi-stage pseudo-labels (PBS without node centrality), and ground truth labels (true labels). The “k-means” and “community detection” variants only consider node features and graph topology respectively. Compared with these two variants, we conclude that graph topology is more important for PBS of GCL. This aligns with the observation that PBS using node centrality information (GBT+ImGCL) significantly outperforms ordinary PBS (GBT+PBS), which also shows that the proposed node centrality (PageRank centrality) is an effective component in PBS. Moreover, ImGCL achieves better or comparable results compared to the variant with true labels, which means that ImGCL indeed generates faithful pseudo-labels from the learned representations in an iterative manner. Overall, ImGCL substantially outperforms the baseline in terms of overall accuracy and improves the performance in few- and medium-shots categories by a large margin at cost of slightly sacrificing the accuracy on many-shots.

Table 3: Ablation studies on the proposed components of ImGCL. We conduct experiments on Amazon-Computers based on the GBT model. *Many*, *Medium*, and *Few* are split according to the number of classes in decreasing order.

	<i>Many</i>	<i>Medium</i>	<i>Few</i>	All
GBT	72.84 \pm 5.96	29.13 \pm 3.58	7.30 \pm 3.65	39.06 \pm 3.67
+K-means	57.67 \pm 9.44	81.25 \pm 8.82	91.57 \pm 10.20	75.99 \pm 6.75
+Community detection	62.47 \pm 8.30	82.1 \pm 8.64	92.33 \pm 9.22	76.57 \pm 3.87
+PBS	55.27 \pm 9.13	79.48 \pm 9.30	96.00\pm6.49	76.70 \pm 6.94
+ImGCL (ours)	58.17 \pm 7.29	83.88\pm8.46	94.67 \pm 6.07	78.62\pm1.73
+True labels	66.83\pm8.37	80.68 \pm 10.55	92.47 \pm 11.76	78.36 \pm 2.89
GBT over GBT+ImGCL	14.67\downarrow	54.75\uparrow	87.37\uparrow	39.56\uparrow

E Hyperparameter Study

We study the hyperparameter sensitivity of our proposed framework ImGCL, and conduct experiments on Amazon-Computers based on the GCN model. We have one main hyperparameter in ImGCL: the re-balanced labeling frequency B . The $\#Labeling = T/B$ denotes the number of stages in which class distribution is re-balanced based on newly-generated pseudo-labels. As the $\#Labeling$ varies from 6 to 12, our proposed ImGCL achieves relatively stable performance. We can also find that when $\#Labeling$ is larger than 10, the accuracy slightly decreases but the variance largely increases. We conjecture that when we produce pseudo-labels frequently, the GCL model cannot quickly adapt to the new sample distribution, which leads to large fluctuations in performance. In summary, we find the performance of our framework is relatively stable across different values of hyperparameter $\#Labeling$.

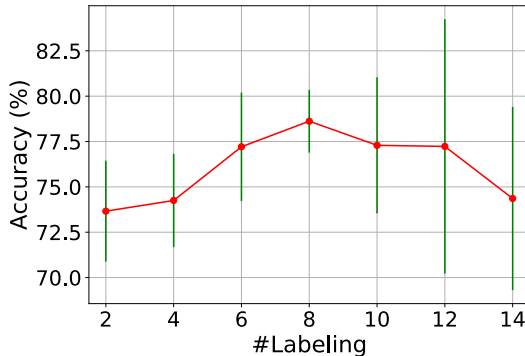


Figure 5: Hyperparameter study on Amazon-Computers.

F Experimental Setup

For reproducibility, we provide all websites of the baseline GNN models and datasets. Our codes and data are publicly available³.

F.1 Experimental Settings

All experiments are conducted with the following settings:

- Operating system: Linux Red Hat 4.8.2-16
- CPU: Intel(R) Xeon(R) Platinum 8255C CPU @ 2.50GHz
- GPU: NVIDIA Tesla V100 SXM2 32GB

³<https://tinyurl.com/ImGCL>

Table 4: Statistics of datasets. The imbalanced ratio is calculated on the entire graph dataset.

	Amazon-Computers	Amazon-Photo	Wiki-CS	DBLP
#Nodes	13752	7650	11701	17716
#Edges	245861	119081	216123	105734
#Features	767	745	300	1639
#Classes	10	8	10	4
#Train	1375	765	1170	1772
#Val per class	20	20	20	150
#Test per class	200	200	200	1500
Imbalanced ratio	17.73	5.86	9.08	4.00

- Software versions: Python 3.8.10; Pytorch 1.9.0+cu102; Numpy 1.20.3; SciPy 1.7.1; Pandas 1.3.4; scikit-learn 1.0.1; PyTorch-geometric 2.0.2; DGL 0.7.2; Open Graph Benchmark 1.3.2

F.2 Datasets

The statistics of datasets we used in experiments are summarized in 4. We also provide a brief description of datasets in the experiment section as follows:

- **Wiki-CS** [1] is a reference network constructed based on Wikipedia. The nodes represent articles about computer science and the edges represent the hyperlinks between two articles. Each node corresponds to a label representing a branch of the field. Node features are calculated by the average of word embeddings in each article.
- **Amazon-Computers** and **Amazon-Photo** [11] are two networks of co-purchase relationships constructed from Amazon. The nodes represent goods and the edges indicate that two goods are frequently bought together. Node features are bag-of-words encoded product reviews, and class labels are given by the product category.
- **DBLP** [11] is a citation network constructed from DBLP website. The nodes represent papers and the edges represent the citation relationship between two papers. For each paper, a sparse bag-of-words vector is utilized as the node feature vector. The node labels are defined according to their research topic.

F.3 Baselines

The publicly available implementations of graph contrastive learning (GCL) baselines and their hyperparameters can be found at the following URLs:

- PyGCL: <https://github.com/GraphCL/PyGCL>
- DGI: <https://github.com/PetarV-/DGI>
- MVGRL: <https://github.com/kavehhassani/mvgrl>
- InfoGraph: <https://github.com/fanyun-sun/InfoGraph>
- GRACE: <https://github.com/CRIPAC-DIG/GRACE>
- BGRL: https://github.com/Namkyeong/BGRL_Pytorch
- GBT: <https://github.com/pbielak/graph-barlow-twins>

G Preliminaries of GNN Encoders

Typically, the training process of modern GNN encoders follows the message-passing mechanism [45] in graph contrastive learning (GCL). During each message-passing iteration, a hidden embedding $\mathbf{h}_u^{(k)}$ corresponding to each node $u \in \mathcal{V}$ is updated by aggregating information from u 's

neighborhood $\mathcal{N}(u)$, which can be expressed as follows:

$$\begin{aligned} \mathbf{h}_u^{(k+1)} &= \text{UPDATE}^{(k)}\left(\mathbf{h}_u^{(k)}, \text{AGGREGATE}^{(k)}\left(\left\{\mathbf{h}_v^{(k)}, \forall v \in \mathcal{N}(u)\right\}\right)\right) \\ &= \text{UPDATE}^{(k)}\left(\mathbf{h}_u^{(k)}, \mathbf{m}_{\mathcal{N}(u)}^{(k)}\right), \end{aligned} \quad (24)$$

where UPDATE and AGGREGATE are arbitrary differentiable functions (*i.e.*, neural networks), and $\mathbf{m}_{\mathcal{N}(u)}$ denotes the “message” that is aggregated from u ’s neighborhood $\mathcal{N}(u)$. The initial embedding at $k = 0$ is set to the input features, *i.e.*, $\mathbf{h}_u^{(0)} = x_u, \forall u \in \mathcal{V}$. After running k iterations of the GNN message-passing, we can obtain information from k -hops neighborhood nodes. Different GNNs can be obtained by choosing different UPDATE and AGGREGATE functions. For example, the classical Graph Convolutional Networks (GCN) [30] updates the hidden embedding as

$$\mathbf{H}^{(l+1)} = \sigma\left(\hat{\mathbf{A}}\mathbf{H}^{(l)}\mathbf{W}^{(l)}\right), \quad (25)$$

where $\mathbf{H}^{(l+1)} = [\mathbf{h}_1^{(l+1)}; \dots; \mathbf{h}_n^{(l+1)}]$ is the hidden matrix of the $(l+1)$ -th layer. $\hat{\mathbf{A}} = \hat{\mathbf{D}}^{-1/2}(\mathbf{A} + \mathbf{I})\hat{\mathbf{D}}^{-1/2}$ is the re-normalization of the adjacency matrix, and $\hat{\mathbf{D}}$ is the corresponding degree matrix of $\mathbf{A} + \mathbf{I}$. $\mathbf{W}^{(l)} \in \mathbb{R}^{C_l \times C_{l+1}}$ is the filter matrix in the l -th layer with C_l referring to the size of l -th hidden layer and $\sigma(\cdot)$ is a nonlinear function, *e.g.*, ReLU.